

# Mobility lifetime product—A tool for correlating *a*-Si:H film properties and solar cell performances

N. Beck, N. Wyrsh, Ch. Hof, and A. Shah

*Institut de Microtechnique, Université de Neuchâtel, Rue A.-L. Breguet 2, CH-2000 Neuchâtel, Switzerland*

The missing correlation between film characteristics and *a*-Si:H-based *p-i-n* solar cells is still a controversial subject. The authors present a new parameter  $\mu^0\tau^0$ , evaluated from steady-state transport measurements on *a*-Si:H layers, which can indeed relate film quality and cell performance as far as the latter is limited by the quality of the intrinsic  $\langle i \rangle$  layer. Thereby, two specific features of the evaluated  $\mu^0\tau^0$  product can explain its successful role as a quality parameter for *a*-Si:H: First, the computation of  $\mu^0\tau^0$  takes into account the effects of the prevailing dangling bond occupation, which is very different in uniform films as compared to the occupation profile prevailing through the *i* layer of a *p-i-n* solar cell; second, the evaluated  $\mu^0\tau^0$  product combines information about band mobility and defect density; furthermore it avoids some of the well-known pitfalls of usual deep defect density measurements such as constant photocurrent method and photothermal deflection spectroscopy. Experimental data on a series of layers and *p-i-n* solar cells illustrates the determination of  $\mu^0\tau^0$  in a given practical case and its successful correlation with cell efficiency. In this context, an estimation for the ratio of charged to neutral capture cross sections  $\sigma^\pm/\sigma^0$  of around 50 is found.

## I. INTRODUCTION

The extensive knowledge about the physics of *a*-Si:H material gained in recent years through research in the field of material characterization has, so far, not really succeeded in improving *a*-Si:H-based solar cells. On the contrary, a lack of correlation between the characteristics measured on *a*-Si:H films and the performances of solar cells made of these materials persists.<sup>1-3</sup>

The aim of the present article is to show that such a correlation can indeed be found. Choosing from a multitude of parameters and characterization methods, the authors show that a particular mobility-lifetime product  $\mu^0\tau^0$  can successfully be used as a parameter for comparing *a*-Si:H layers and solar cells. Physically, this new product of band mobility ( $\mu^0$ )  $\times$  capture time ( $\tau^0$ ) corresponds to the value that the  $\mu\tau$  product (measured in an *a*-Si:H layer) would take if all defects in the material were neutral.

Thereby, several important aspects account for our choice of this specific product  $\mu^0\tau^0$  as a correlation parameter between layers and solar cells. First, the product  $\mu^0\tau^0$  is independent of dangling bond occupation. As the prevailing dangling bond occupation in an *a*-Si:H film has little in common with the strongly inhomogeneous distribution of dangling bond charge through the intrinsic layer of a *p-i-n* solar cell (related to the internal electric field), this is a necessary condition. Second the product  $\mu^0\tau^0$  combines information about defect density and band mobility; this is a definite advantage over the usual measurements on the deep defect density alone. Third the product  $\mu^0\tau^0$  is closely related to the performances of *a*-Si:H-based solar cells, as far as the latter is controlled by the quality of the intrinsic layer. Last, but not least, the evaluation of  $\mu^0\tau^0$  does not suffer from the known drawbacks of deep defect density measurements, namely, the limitations in photothermal deflection spectroscopy (PDS)<sup>4</sup> and constant photocurrent method (CPM) (the latter mainly

in the case of intrinsic or *p*-type samples).<sup>5-7</sup>

As normally both neutral and charged defects exist in *a*-Si:H material, the value of  $\mu^0\tau^0$  is generally masked and cannot be measured directly. Nevertheless, and this represents an important point here, we show that this correlation parameter  $\mu^0\tau^0$  can be deduced by combining steady-state photoconductivity (SSPC) and steady-state photocarrier grating (SSPG) measurements. In the framework of the mono-molecular recombination model via dangling bonds, we present an ‘‘easy to use’’ procedure for evaluating the value of  $\mu^0\tau^0$  from experimental data. The validity as well as the limits of the method is also discussed in Sec. II F.

In Sec. IV of this article we present the results obtained by applying our procedure to different series of undoped *a*-Si:H layers of variable quality, the latter being modified by changing the deposition temperature and by degrading the material. Thereby, we compare the  $\mu^0\tau^0$  products evaluated on these films with the performances of standard *p-i-n* solar cells which incorporate the ‘‘same’’ undoped material (i.e., material obtained using the same deposition parameters) as an active, intrinsic  $\langle i \rangle$  layer. The correlation between  $\mu^0\tau^0$  products evaluated on films and the conversion efficiencies of the corresponding solar cells are discussed.

## II. THE EVALUATION AND USE OF $\mu^0\tau^0$ PRODUCTS IN *a*-Si:H

$\mu\tau$  products are commonly used for the characterization of transport properties of *a*-Si:H layers. These  $\mu\tau$  products are band mobility  $\times$  recombination time products (when evaluated from steady-state measurements) or band mobility  $\times$  deep-trapping time products [i.e., in the case of time-of-flight (TOF) measurements]; however, in both cases they strongly depend on the prevailing dangling bond occupation in the film.<sup>8-10</sup> As the charge state of these deep defects is not a material constant but significantly varies with inten-

tional or unintentional doping or with illumination, the results obtained by these techniques describe correctly the properties of the measured film, but do not give correct information about the behavior of the same material in a  $p-i-n$  solar cell, where the distribution of charged dangling bonds is related to the internal electric field. Therefore, a  $\mu\tau$  product (we call it  $\mu^0\tau^0$ ) that is independent of the charge state of deep defects is more adequate to describe the properties of both films and cells. In this section we show how  $\mu^0\tau^0$  can be evaluated from SSPC and SSPG measurements. A short description of this approach has already been presented elsewhere.<sup>11</sup>

For our analysis we will consider  $a$ -Si:H material at room temperature and under steady-state illumination, where the precise energetical position and distribution of the dangling bond states have virtually no influence and where the thermal emissions from deep defects as well as recombination by band-tail states can be neglected. In this domain, the model of bimolecular recombination through dangling bonds<sup>12,13</sup> is valid: Free carriers only recombine through the dangling bond states. In this case, the charge state of dangling bonds will, thus, exclusively be determined by the recombination kinetics of electrons and holes.

Consequently, the recombination traffic of electrons (monitored by SSPC) and holes (monitored by SSPG) are not independent of each other, but they are related via the density and charge state of their common recombination centers, the dangling bond states. Experimentally, this fact can be observed as an anticorrelated behavior of electron and hole transport properties.<sup>10,9</sup> For the evaluation of  $\mu^0\tau^0$ , we take advantage of this fact. Under steady-state conditions, where the above-mentioned conditions are valid, this link between electron and hole  $\mu\tau$  products can be expressed analytically. This makes it possible to work out the influence of the dangling bond occupation on the experimentally measured  $\mu\tau$  products. From there on, simple mathematical manipulation leads to the evaluation of the dangling bond independent  $\mu^0\tau^0$  product.

### A. Definition of the correlation parameter $\mu^0\tau^0$

The correlation parameter for  $a$ -Si:H layers and solar cells is defined as a band mobility ( $\mu^0$ )  $\times$  capture time ( $\tau^0$ ) product. As already mentioned, it represents the value which the measured  $\mu\tau$  product would take if only neutral dangling bonds existed in the material (indicated by the superscript 0 of the parameter  $\tau^0$ ). Thereby, we assume that  $\mu^0\tau^0$  is equal for electrons and holes,

$$\mu_n^0\tau_n^0 = \mu_p^0\tau_p^0 = \mu^0\tau^0. \quad (1)$$

This simplification can be justified on the basis of earlier TOF measurements performed by us, on compensated (fully intrinsic, i.e., ‘‘midgap’’)  $a$ -Si:H samples, as well as on degraded  $a$ -Si:H samples.<sup>9,14</sup> In these two cases, we have reason to assume that almost all dangling bonds in the material are neutral and, consequently, the experimentally measured  $\mu\tau$  products approach the stated ‘‘dangling bond charge independent’’  $\mu^0\tau^0$  product for both carriers, electrons, and holes. The TOF measurements just cited<sup>9,14</sup> revealed experimentally that  $\mu_n^0\tau_n^0$  and  $\mu_p^0\tau_p^0$  are almost equal:

$\mu_n^0\tau_n^0/\mu_p^0\tau_p^0 \approx 1.2$ . (The values  $\mu_n^0\tau_n^0/\mu_p^0\tau_p^0 = 3-5$  given in our earlier articles are wrong; they were incorrectly deduced from the correct experimental data.) Note that in the particular situation where no charged dangling bonds exist in the material, the  $\mu\tau$  products obtained by TOF experiments and by SSPC/SSPG are equivalent.<sup>9,14</sup>

This experimental result is also comprehensive from basic physical considerations: In a given  $a$ -Si:H layer, the carrier with higher velocity (electrons) has an enhanced mobility, but also a proportionally reduced capture time compared to the carrier with lower free carrier velocity (holes). This leads, thus, to the same  $\mu^0\tau^0$  product for holes and electrons.

### B. Photoconductivity (SSPC) and steady-state photocarrier grating (SSPG)

As described above, the  $\mu^0\tau^0$  product is evaluated from the results which can be obtained from SSPC and SSPG measurements. In these measurement techniques, a steady-state situation between generation and recombination of free carriers is achieved by illuminating the sample. Details on the experimental methods can be found elsewhere (e.g., Refs. 15 or 16). As is well known and widely accepted, the measured photoconductivity  $\sigma_{ph}$  (from SSPC) and ambipolar diffusion length  $L_{amb}$  (from SSPG) can be connected to  $\mu\tau$  products using the following (or equivalent) expressions:

$$\sigma_{ph} = e(\mu_n^0 n_f + \mu_p^0 p_f) = eG(\mu_n^0 \tau_n^R + \mu_p^0 \tau_p^R), \quad (2)$$

$$L_{amb}^2 = \frac{kT}{e} \frac{\mu_n^0 \tau_n^R \mu_p^0 \tau_p^R}{\mu_n^0 \tau_n^R + \mu_p^0 \tau_p^R} C, \quad (3)$$

where  $\mu_n^0 \tau_n^R$  and  $\mu_p^0 \tau_p^R$  are band mobility  $\times$  recombination time products for electrons and holes, respectively;  $kT$  is the thermal energy,  $e$  is the elementary charge, and  $C$  is a constant having a value between 1 and 2 (Ref. 17).

Additional information about the  $n$  or  $p$ -type character of a material can be gained by combining both  $L_{amb}$  and  $\sigma_{ph}$  through a parameter  $b$ , which reflects the position of the two quasi-Fermi levels  $E_{Fn}$  and  $E_{Fp}$  with respect to the midgap. Introduced in Ref. 16, the parameter  $b$  is defined as

$$b = \frac{\mu_n^0 n_f}{\mu_p^0 p_f} = \frac{\mu_n^0 \tau_n^R}{\mu_p^0 \tau_p^R}. \quad (4)$$

The parameter  $b$  can be deduced using either the above definition (4) (for extrinsic material) or the following expression [deduced from Eqs. (2) and (3)]:

$$\frac{b}{(b+1)^2} = \frac{L_{amb}^2 e^2 G}{kT \sigma_{ph} C}. \quad (5)$$

Under steady-state illumination (with the mentioned conditions) the recombination times for electrons and holes in the expressions (2) and (3) can be written as

$$\tau_n^R = \frac{1}{v_{th} N_{db} \sigma_n^0 f^0 + v_{th} N_{db} \sigma_n^+ f^+}, \quad (6)$$

$$\tau_p^R = \frac{1}{v_{th} N_{db} \sigma_p^0 f^0 + v_{th} N_{db} \sigma_p^- f^-}, \quad (7)$$

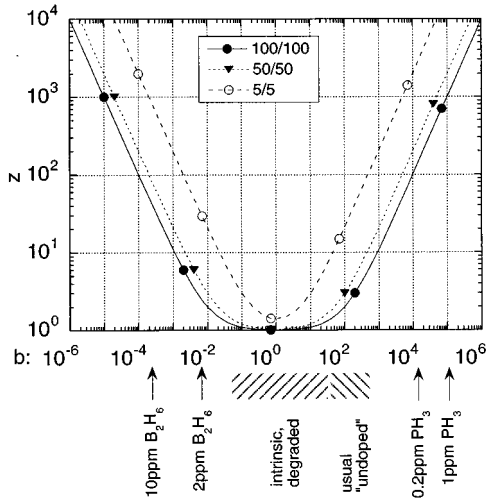


FIG. 1. Calculated magnitude of the correction factor  $z$  for experimental  $\mu^0\tau^0$  products deduced from photoconductivity (see below) with different values of the parameter  $b$ ; the correction factor  $z$  is used in order to obtain the new “quality-related”  $\mu^0\tau^0$  products. The box indicates the different ratios of capture cross sections  $\sigma_n^+/\sigma_n^0$  and  $\sigma_p^-/\sigma_p^0$  used for this calculation. In the horizontal axis, some typical experimental values of the parameter  $b$  for undoped, degraded, and slightly doped  $a$ -Si:H layers are indicated.

where  $v_{th}$  is thermal velocity,  $N_{db}$  is the deep defect density,  $\sigma_n^0, \sigma_n^+, \sigma_p^0, \sigma_p^-$  are the capture cross sections of the dangling bonds, and  $f^0, f^-, f^+$  are the dangling bond occupation functions. The latter can be expressed in the following simple form:<sup>12,13</sup>

$$f^0 = \frac{1}{(p_f/n_f)(\sigma_p^0/\sigma_n^+) + 1 + (n_f/p_f)(\sigma_n^0/\sigma_p^-)}, \quad (8)$$

$$f^- = \frac{(n_f/p_f)(\sigma_n^0/\sigma_p^-)}{(p_f/n_f)(\sigma_p^0/\sigma_n^+) + 1 + (n_f/p_f)(\sigma_n^0/\sigma_p^-)}, \quad (9)$$

$$f^+ = \frac{(p_f/n_f)(\sigma_p^0/\sigma_n^+)}{(p_f/n_f)(\sigma_p^0/\sigma_n^+) + 1 + (n_f/p_f)(\sigma_n^0/\sigma_p^-)}. \quad (10)$$

Note that, thanks to the steady-state illumination,  $f^0, f^-$ , and  $f^+$  exclusively depend on the free carrier density which is monitored by the  $\sigma_{ph}$  and  $L_{amb}$  measurements. The influence of the dangling bond occupation on  $\mu\tau$  products can thus be evaluated without involving any further experimental method (other than SSPC and SSPG).

### C. Evaluation of the product $\mu^0\tau^0$ from SSPC and SSPG measurements

Combining the different elements (2)–(10) of Sec. II B one can deduce a simple relationship between the experimentally determined quantities ( $\sigma_{ph}$ ,  $b$ ) and the correlation parameter  $\mu^0\tau^0$ ,<sup>11</sup>

$$\mu^0\tau^0 = \frac{\sigma_{ph}}{eG} \frac{1}{z}, \quad z = \frac{1}{f^0} = \left( \frac{\sigma_n^0}{\sigma_n^+} \frac{1}{b} + 1 + \frac{\sigma_p^0}{\sigma_p^-} b \right). \quad (11)$$

In Fig. 1 the magnitude of the correction factor  $z$  (for given ratios  $\sigma_n^0/\sigma_n^+$  and  $\sigma_p^0/\sigma_p^-$ ) is plotted as a function of the parameter  $b$ . Some typical ranges for the value of the parameter  $b$  are also indicated.

From the same figure one can see that only for truly intrinsic material (Fermi energy level near midgap), with  $b$  close to unity, the correction factor  $z$  is approximately 1. This means that only for these particular  $a$ -Si:H materials (i.e., degraded or “compensated”  $a$ -Si:H) the measured value of the photoconductivity  $\sigma_{ph}$  directly monitors the film quality and can be used to correlate layer properties with solar cells. In all other cases where the investigated  $a$ -Si:H layer exhibits a certain extrinsic behavior ( $b$  substantially different from 1), the measured measured value of the photoconductivity does no longer monitor material properties and the correction factor  $z$  must be evaluated with the help of the measurement of  $L_{amb}$ . The undoped, but slightly  $n$ -type  $a$ -Si:H material produced by standard glow discharge (GD) deposition techniques typically fits (in the annealed state) into this second category and one can show for this material that the  $\mu^0\tau^0$  product becomes proportional to  $L_{amb}$ . Note, however, that with nonstandard deposition techniques such as hot-wire deposition or GD with hydrogen dilution the Fermi level of the resulting layers may vary in a large range; therefore, special care has to be taken.

### D. Estimation of the ratio of the capture cross sections

Up to now we have presented a simple evaluation method for the the correlation parameter  $\mu^0\tau^0$ ; however, there is one problem which remains to be solved before  $\mu^0\tau^0$  can be easily used in practice: The ratios of the capture cross sections  $\sigma_n^+/\sigma_n^0$  and  $\sigma_p^-/\sigma_p^0$  which appear in our Eq. (11) are not very well known. The values given in literature vary between 1.8 (Ref. 18) and  $\geq 100$ ,<sup>19,20</sup> and are still a subject of discussion. As it is this value that defines the limits between midgap material and extrinsic  $a$ -Si:H, we address this subsection to the estimation of the ratio of capture cross sections.

We performed two different experiments on 2.2–3.8- $\mu\text{m}$ -thick  $a$ -Si:H layers: We measured the variation of  $\mu^0\tau^0$  with light soaking and with low level doping (“microdoping”). Assuming the  $\mu^0\tau^0$  product to be proportional to  $1/N_{db}$  (i.e. the band mobility is not substantially changed by doping or degradation<sup>21</sup>), one can deduce from these experiments an approximate ratio of the capture cross sections. The samples used for these measurements were produced by the very high frequency glow discharge (VHF-GD) deposition technique (70 MHz)<sup>22</sup> on glass substrate (Corning 7059) and provided with two coplanar aluminium contacts of 0.5 mm gap spacing.

#### 1. Microdoping

It is a well-documented fact that even slight doping dramatically changes the transport properties of  $a$ -Si:H layers,<sup>23</sup> i.e., a steep increase of photoconductivity is observed. On the other hand, the corresponding change in the deep defect density is much lower and has experimentally be found to follow a  $1/\sqrt{[\text{dopant}]/[\text{SiH}_4]}$  law<sup>23</sup> and, according to the above argumentation, also the  $\mu^0\tau^0$  product evaluated on a series of  $a$ -Si:H samples should reproduce this  $1/\sqrt{[\text{dopant}]/[\text{SiH}_4]}$  dependency for a correctly chosen ratio of capture cross sections (see Fig. 2).

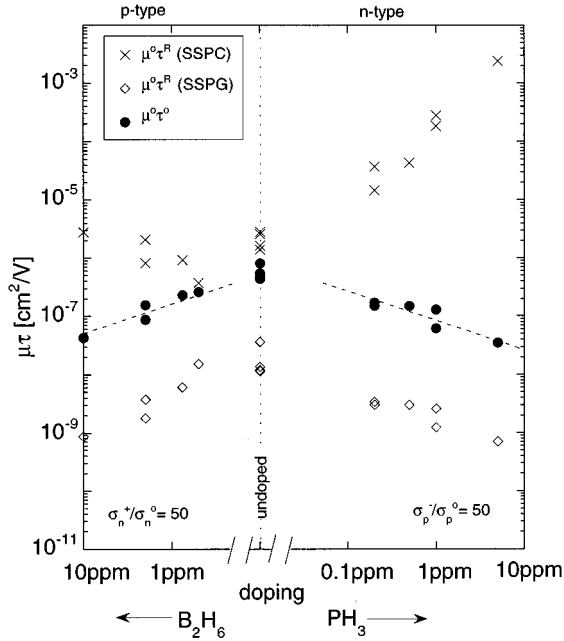


FIG. 2. Variation in the direct experimental products  $\mu_n^0\tau_n^R$ ,  $\mu_p^0\tau_p^R$ , and of the deduced quality-related  $\mu^0\tau^D$  product as a function of low-level  $\text{PH}_3$  and  $\text{B}_2\text{H}_6$  doping. A ratio of capture cross sections  $\sigma_n^+/\sigma_n^0$  and  $\sigma_p^-/\sigma_p^0$  of 50 was chosen for the plot. The  $1/\sqrt{[\text{B}_2\text{H}_6]/[\text{SiH}_4]}$  law is indicated by the dotted lines.

For  $p$ -type samples, a  $1/\sqrt{[\text{dopant}]/[\text{SiH}_4]}$  behavior can only be obtained if the ratio  $\sigma_n^+/\sigma_n^0$  is adjusted to around 50 (with a tolerance of about a factor of 2). On the other hand, for  $n$ -type samples, even a very slight doping pushes the Fermi level far away from midgap which results in almost all dangling bonds being doubly occupied ( $D^-$ ). Consequently the ratio of capture cross sections  $\sigma_p^-/\sigma_p^0$  is not a critical parameter, in this case, and no information about it can be deduced from such  $n$ -type samples.

## 2. Light soaking

For the light soaking experiment, an undoped but initially slightly  $n$ -type  $a$ -Si:H layer was stepwise degraded with a Krypton laser ( $\lambda=647$  nm) at a power density of about  $100$  mW/cm<sup>2</sup>. After each step SSPC, SSPG, and CPM were measured (Fig. 3). The very initial part of degradation, which was accompanied by a decrease of dark conductivity, was omitted as it was shown that CPM may not measure correctly the absorption spectra in this case.<sup>5,6</sup> While degrading further, the dark conductivity remained constant and the absorption at  $1.2$  eV was then used as a monitor for the deep defect density. Then, the mutual change of  $\mu\tau$  products deduced from SSPC and SSPG measurements was fitted with different values for the ratio of capture cross sections  $\sigma_p^-/\sigma_p^0$  and, thereafter, the resulting  $\mu^0\tau^D$ , which is expected to decrease proportionally to the increase of  $\alpha_{\text{CPM}}$  ( $1.2$  eV), was evaluated. The best fit with a  $\mu^0\tau^D$  proportional to  $1/\alpha_{\text{CPM}}$  ( $1.2$  eV) (see Fig. 3) was obtained for  $\sigma_p^-/\sigma_p^0 \approx 50$  (with a tolerance of about a factor of 2).

As previous work had shown that CPM does not correctly measure the absorption spectra for slightly  $p$ -type

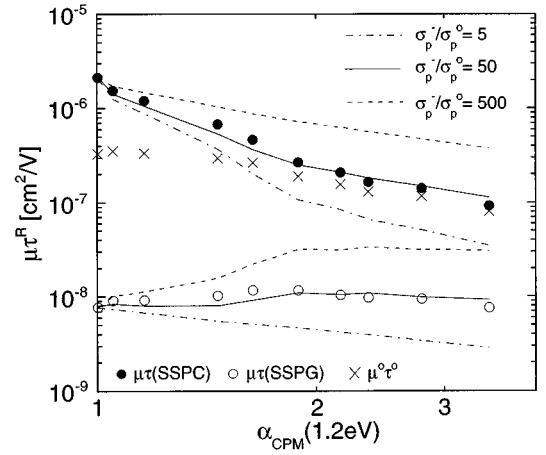


FIG. 3. Variation of the direct experimental products  $\mu_n^0\tau_n^R$ ,  $\mu_p^0\tau_p^R$ , and in the corresponding quality-related  $\mu^0\tau^D$  products evaluated therefrom, for an undoped,  $2.4$ - $\mu\text{m}$ -thick  $a$ -Si:H film, as a function of the increasing deep defect density, during the process of light soaking, the latter being monitored by measuring CPM absorption at  $1.2$  eV. The best fit was obtained by using a ratio of capture cross sections  $\sigma_p^-/\sigma_p^0=50$ ; the points marked by  $\times$  indicate the corresponding  $\mu^0\tau^D$  product (for  $\sigma_p^-/\sigma_p^0=50$ ) which is now almost proportional to  $1/\alpha_{\text{CPM}}$  ( $1.2$  eV).

samples,<sup>5</sup> no similar experiments were carried out for such samples (in order to find  $\sigma_n^+/\sigma_n^0$ ).

As a conclusion of this section, the two experiments of microdoping and light soaking allowed us to make a rough estimation of the ratios of capture cross sections of about  $\sigma_p^-/\sigma_p^0 \approx \sigma_n^+/\sigma_n^0 \approx 50$ . This value will be used in Sec. IV of this article.

## E. About the practical use of $\mu^0\tau^D$

As shown in Sec. II C, the correlation parameter  $\mu^0\tau^D$  can easily be evaluated for all types of  $a$ -Si:H layers from SSPC and SSPG measurements, with the help of expression (11). However, the arguments of Sec. II D lead to a direct

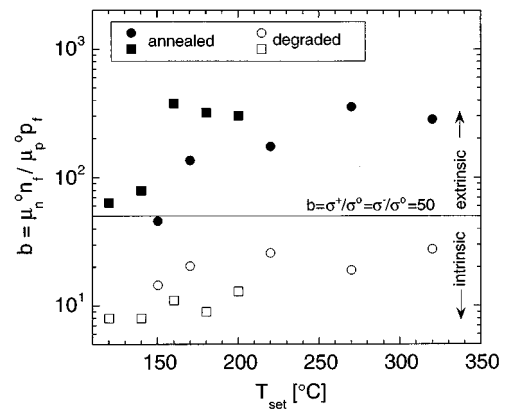


FIG. 4. Variation in the value of the parameter  $b$  with light-induced degradation for the two temperature series (circle and squares) of undoped layers: While in the annealed state almost all materials are shown to have a slightly extrinsic character they all become truly intrinsic (midgap) with light soaking. The limit between extrinsic and truly intrinsic is given (according to our above definition, see Table I) by the ratio of capture cross sections  $\sigma^-/\sigma^0$ , which was estimated to be 50.

TABLE I. Evaluation recipes for determining the product  $\mu^0\tau^0$  in  $n$ -type,  $p$ -type, and truly intrinsic  $a$ -Si:H. Note that under the assumptions introduced here, evaluation of  $\mu^0\tau^0$  is particularly simple once the character of the layer is known. Thereby, the ratios of capture cross sections  $\sigma_n^0/\sigma_n^+$  and  $\sigma_p^0/\sigma_p^-$ , as compared to the parameter  $b$ , play the role of a test criterion to differentiate between intrinsic  $a$ -Si:H and material with a certain extrinsic character.

$n$ type	$b > \frac{\sigma_p^-}{\sigma_p^0}$	$\mu^0\tau^0 \approx \mu_p^0\tau_p^R \frac{\sigma_p^-}{\sigma_p^0} \approx L_{\text{amb}}^2 \frac{1}{C} \frac{e}{kT} \frac{\sigma_p^-}{\sigma_p^0}$
Intrinsic	$\frac{\sigma_n^0}{\sigma_n^+} < b < \frac{\sigma_p^-}{\sigma_p^0}$	$\mu^0\tau^0 \approx \frac{\sigma_{\text{ph}}}{eG}$
$p$ -type	$b < \frac{\sigma_n^0}{\sigma_n^+}$	$\mu^0\tau^0 \approx L_{\text{amb}}^2 \frac{e}{kT} \frac{1}{C} \frac{\sigma_n^+}{\sigma_n^0}$

recipe for the practical use: When optimizing undoped, but slightly  $n$ -type,  $a$ -Si:H for solar-cell applications, we must focus (in the annealed state) on an improvement of  $L_{\text{amb}}$  rather than of  $\sigma_{\text{ph}}$ . Such a correlation between  $L_{\text{amb}}$  and solar cell initial (undegraded) performance has indeed already been observed by Li *et al.*<sup>24</sup> On the other side, in the degraded state when  $b$  becomes close to 1, the photoconductivity becomes the correct parameter to describe the quality of  $a$ -Si:H layers and, thus, should be used to correlate layer properties with stabilized (degraded) solar cell performances. Nevertheless, one should always take the precaution to check that the material has really become “truly intrinsic” with light soaking. The different situations where the expression (11) can be simplified are assembled in Table I.

The new correlation parameter  $\mu^0\tau^0$  may also be used to obtain information about the relative stability of an  $a$ -Si:H material during light soaking. Thereby,  $\mu^0\tau^0$  must be evaluated, both in the annealed as well as in the degraded state. Assuming the band mobility to be unchanged by light soaking,<sup>2</sup> the ratio between the  $\mu^0\tau^0$  products in the initial and degraded states becomes an indicator for the increase of the deep defect density,

$$\frac{(\mu^0\tau^0)_{\text{initial}}}{(\mu^0\tau^0)_{\text{degraded}}} \approx \frac{(N_{\text{db}})_{\text{degraded}}}{(N_{\text{db}})_{\text{initial}}}. \quad (12)$$

### F. Validity of the method and its limitations

One of the main points in favor of the evaluation procedure of  $\mu^0\tau^0$ , as presented in Sec. II C, is its simplicity and transparency, however, as several approximations were necessary to obtain the final result (11), let us briefly discuss the validity of the method and its limitations.

The basic assumption of the presented method for the evaluation of the  $\mu^0\tau^0$  product is the dangling bond recombination model. Thus, the validity of our procedure is in principle determined by the range of experimental conditions for which the dangling bond recombination model is a valid approximation. As the validity of the latter has been discussed by different authors (e.g., Refs. 12, 13, 25), it is not repeated here. We just would like to stress the experimental importance of using approximately homogeneously absorbed light (in our case  $\lambda=647$  nm) as well as of a careful choice of the illumination intensity for the measurement of SSPC and SSPG on layers.

Furthermore, as the generally observed nonlinear dependency of the photoconductivity on the generation rate (for undoped, but slightly  $n$ -type  $a$ -Si:H) cannot entirely be explained by the dangling bond recombination model, the evaluated  $\mu^0\tau^0$  in some cases also exhibits a slight dependency on the illumination intensity (power-law exponent between 0 and  $-0.3$ ). For the measurements reported hereafter we always chose a small generation rate which still allowed a correct measurement of the ambipolar diffusion length. This condition was mainly given by a ratio of  $\sigma_{\text{photo}}/\sigma_{\text{dark}}$  of at least 20.

The ratios of capture cross sections determined in Sec. II D are rough estimations and we considered them to be constant for all samples studied here. They fix the limit between intrinsic and extrinsic material and thus play an important role. A more detailed consideration of this point, however, would be desirable in future work.

On the other side, the rather far-reaching assumption (1) was mainly introduced by us in order to gain physical insight. The equalization of  $\mu_n^0\tau_n^0$  and  $\mu_p^0\tau_p^0$  is basically not necessary; omitting it would simply result in an additional constant in the final result (11).

### III. THE ROLE OF $\mu^0\tau^0$ PRODUCTS IN $a$ -Si:H SOLAR CELLS

It is conceptionally quite obvious that in the ideal case a monotonous relation between  $\mu^0\tau^0$  products and the corresponding solar cell performances exists, i.e., that a material with good band mobility and low defect density will lead to a solar cell which well collects the photogenerated carriers. On the other hand, to find a quantitative relationship between the evaluated  $\mu^0\tau^0$  product and the collection or the efficiency of a solar cell is less straightforward because of the rather complex structure and operation of a  $p$ - $i$ - $n$  device. In the expressions used to describe the operation of a solar cell, the band mobility and capture time generally do not appear as a product but individually, which makes simple argumentation difficult. However, in a simplified situation (constant electric field, majority of defects are neutral) a direct relationship between the  $\mu^0\tau^0$  product and the collection  $\chi$  in the solar cell can be established analytically.<sup>13</sup>

Also, a correlation between layer properties (monitored by  $\mu^0\tau^0$ ) and solar-cell efficiencies can obviously only be expected when the latter is governed by the quality of the intrinsic layer. A multitude of other factors (i.e., interface problems, changed absorption properties due to modified bandgap, varying thicknesses, different reflection properties, etc.) can strongly influence the overall efficiency and in such a case the quality of the intrinsic layer will lose its relative importance. However, in these situations, a measurement of the  $\mu^0\tau^0$  product of the  $i$  layer can help to distinguish between problems related to the quality of the intrinsic layer and other structural problems.

### IV. CORRELATION BETWEEN $\mu^0\tau^0$ OF $a$ -Si:H LAYERS AND SOLAR CELL PERFORMANCES

Our dangling bond charge independent  $\mu^0\tau^0$  product was mainly introduced with the aim to create a practical tool for

*a*-Si:H material optimization in view of solar cell applications. Thus, we compare in this section, experimentally, layer properties and the performances of corresponding *p-i-n* solar cells incorporating the same materials as intrinsic layers. Thereby, the products  $\mu^0\tau^0$  are employed to describe the quality of intrinsic *a*-Si:H layers.

### A. Experiment

Two series of pairs, each of them consisting of an *a*-Si:H layer and a thin *p-i-n* solar cell, were produced by the VHF-GD deposition technique;<sup>22</sup> thereby, the deposition set-point temperature was varied from 120 to 320 °C. In this context, first an approximately 2.5- $\mu\text{m}$ -thick, undoped *a*-Si:H film was deposited on a glass substrate and provided with two coplanar, ohmic aluminum contacts. Subsequently, using the same deposition parameters, this *a*-Si:H material was incorporated as an *i* layer (thickness  $\approx 0.6 \mu\text{m}$ ) in a standard *p-i-n* solar cell on glass coated by transparent conductive oxide (TCO) (Asahi type U). Both cells and layers were then annealed for 2 h at 180 °C.

The layers were characterized by transport measurements (SSPC and SSPG), by PDS and by the CPM. For the transport measurements (SSPC and SSPG), a Krypton laser ( $\lambda=647 \text{ nm}$ ) was used. Furthermore, the dark conductivity and the optical band gap (from Tauc's plot) were determined. For the cells, the conversion efficiency  $\eta$ , the open-circuit voltage  $V_{oc}$ , the short-circuit current density  $i_{sc}$ , and the fill factor (FF) were evaluated using a two-source solar simulator (Wacom WXS-140S-10).

The layers were light soaked during 4 weeks by a 6 sun high-pressure sodium lamp [spectral maximum at 590 nm with full width at half-maximum (FWHM) of around 40 nm] at 46 °C. The cells were degraded during 3 weeks by an AM1.5 light source of 100 mW/cm<sup>2</sup> (array of Philips PL-L 24W/95/4P lamps) at 47 °C.

### B. The annealed state

The results obtained in the annealed state, for both series, are recapitulated in Tables II (layers) and III (cells).

In the annealed states, we plotted, as a first feature, the value of the parameter  $b$  as a function of the deposition temperature (Fig. 4). Thereby, assuming a ratio of  $\sigma^\pm/\sigma^0=50$ , all deposited layers (with the exception of the sample deposited at 150 °C) fit into the category of extrinsic material and, consequently, the measured transport properties need to be corrected before the layer properties can be compared to the solar cells. Furthermore, the *n*-type character of the layers slightly increases with increasing deposition temperature.

The  $\mu^0\tau^0$  products deduced for the two series of layers (solid and open circles in Fig. 5) are almost constant for temperatures above 220 °C but decrease steeply for lower temperatures. A similar change with temperature is also seen in the CPM absorption measurements (calibrated by PDS measurements), a technique which was used by us to monitor the deep defect density. Nevertheless, the deterioration of transport quality (as seen by the evaluation of  $\mu^0\tau^0$ ) is much stronger than the increase in deep defect density (as seen by CPM).

TABLE II. Temperature series: Properties of 2.5- $\mu\text{m}$ -thick *a*-Si:H layers in the annealed state and in the degraded state (latter in brackets).

$T_{\text{set}}^a$ (°C)	$b$	$\mu^0\tau^0$ (cm <sup>2</sup> /V)	$\alpha_{\text{CPM}}$ (1.2 eV)
120	64 (8)	$5.7 \times 10^{-8}$ ( $2.4 \times 10^{-9}$ )	0.9 (24)
140	80 (8)	$8.9 \times 10^{-8}$ ( $3.1 \times 10^{-9}$ )	1.0 (16)
150	46 (15)	$4.2 \times 10^{-8}$ ( $6.1 \times 10^{-9}$ )	1.4 (6)
160	376 (11)	$1.2 \times 10^{-7}$ ( $7.7 \times 10^{-9}$ )	0.3 (12)
170	136 (20)	$1.9 \times 10^{-7}$ ( $1.6 \times 10^{-8}$ )	0.9 (6.5)
180	320 (9)	$1.7 \times 10^{-7}$ ( $8.3 \times 10^{-9}$ )	0.4 (10)
200	303 (13)	$2.6 \times 10^{-7}$ ( $1.8 \times 10^{-8}$ )	0.2 (12)
220	175 (26)	$3.5 \times 10^{-7}$ ( $3.6 \times 10^{-8}$ )	0.4 (4)
270	355 (19)	$3.5 \times 10^{-7}$ ( $4.8 \times 10^{-8}$ )	0.4 (3.5)
320	283 (28)	$3.6 \times 10^{-7}$ ( $4.8 \times 10^{-8}$ )	0.4 (4)

<sup>a</sup> $T_{\text{set}}$  indicates the set-point temperature. Actual substrate temperature is about 20 °C ( $T_{\text{set}}=150$  °C) to 60 °C ( $T_{\text{set}}=320$  °C) lower than the set-point temperature.

The solar cells incorporating these materials as *i* layers show a similar strong decrease of performances for deposition temperatures below 220 °C (Fig. 5). On the other hand, the cell efficiencies also deteriorate for higher deposition temperatures. Nevertheless, at these high temperatures inter-diffusion problems may become important and even dominant in limiting cell performance. In accordance with this hypothesis, the short-circuit current density  $j_{sc}$ , which remains high even at high deposition temperatures, does not indicate any major deterioration of the intrinsic layer.

### C. The light soaked state

The properties measured on layers and cells after light soaking are listed in brackets in Tables II and III.

In the degraded state the values of the parameter  $b$  for all films are strongly reduced and, according to our above definition (with the limit between extrinsic and intrinsic films given by a cross-section ratio of  $\sigma^\pm/\sigma^0=50$ ), all *a*-Si:H layers have become ‘truly’ intrinsic (i.e., midgap) (see Fig. 4). CPM measurements performed after degradation (see Table II) show, here again, a less-pronounced increase at low temperatures compared to the deterioration of  $\mu^0\tau^0$  products.

### D. Correlation between layer properties and cell performances

The correlation between the layer properties (monitored by our correlation parameter  $\mu^0\tau^0$ ) and the solar cell conver-

TABLE III. Temperature series: Solar cell performance in the annealed state and in the degraded state (latter in brackets).

$T_{\text{set}}$ of <i>i</i> layer	$\eta$ (%)	FF	$j_{sc}$ (mA/cm <sup>2</sup> )	$V_{oc}$ (V)
120	6.9 (1.1)	0.60 (0.30)	13.5 (4.9)	0.850 (0.786)
140	7.2 (2.3)	0.65 (0.35)	13.4 (8.1)	0.825 (0.796)
150	7.1 (3.2)	0.55 (0.37)	16.2 (11.2)	0.788 (0.787)
160	8.9 (3.1)	0.66 (0.38)	15.6 (10.2)	0.859 (0.816)
170	9.6 (4.9)	0.65 (0.46)	16.5 (12.7)	0.852 (0.828)
180	9.1 (3.7)	0.69 (0.41)	15.4 (11.0)	0.855 (0.830)
200	9.7 (5.4)	0.71 (0.48)	16.0 (13.5)	0.851 (0.826)
220	10.3 (6.5)	0.67 (0.52)	18.0 (15.1)	0.848 (0.835)
270	9.5 (6.7)	0.65 (0.54)	18.0 (15.2)	0.827 (0.821)
320	8.3 (6.5)	0.60 (0.52)	17.6 (15.9)	0.781 (0.785)

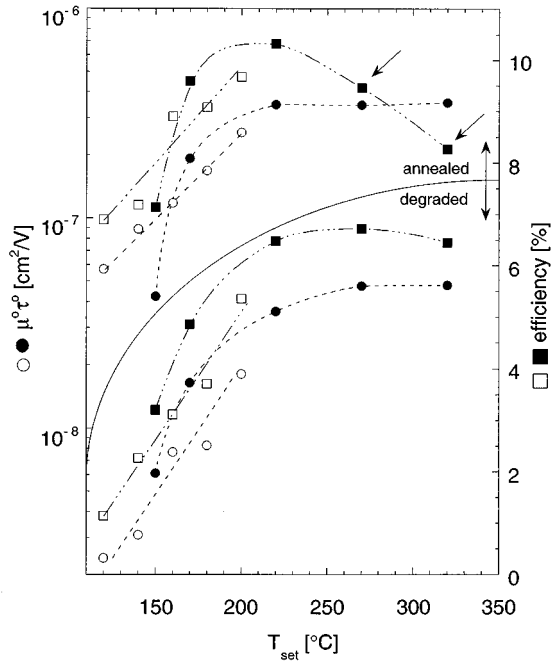


FIG. 5. Correlation between the  $\mu^0\tau^0$  products evaluated on a series of 2.5- $\mu\text{m}$ -thick, undoped layers, on one side, and efficiencies of solar cells incorporating the “same” material as an  $i$  layer on the other side; results are given for both the annealed and the degraded state. The two cell efficiencies for high-temperature deposition (as marked by arrows) are presumably reduced due to interdiffusion problems.

sion efficiencies are plotted in Fig. 6. Additionally to the data obtained in the annealed state, we also plotted the results after degradation, even though the layers and cells were light soaked by different light sources. Figure 6 must thus be interpreted as composed by two parts: the correlation in the annealed state (solid symbols) and in the degraded state (open symbols).

The correlation obtained between the  $\mu^0\tau^0$  products of the layers and the efficiencies of the corresponding solar

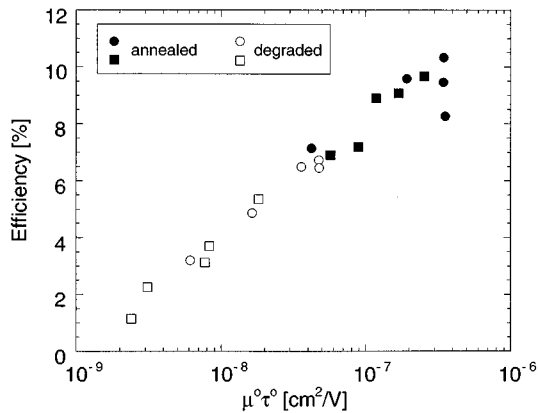


FIG. 6. Correlation between  $\mu^0\tau^0$  products evaluated on two series (squares and circles) of layers and the corresponding solar cell efficiencies in the annealed and in the degraded state (same data as in Fig. 5, but different graphical representation). Note that cells and layers were degraded differently and thus the graph must be considered to be composed of two independent parts: annealed state (solid symbols) and degraded state (open symbols).

cells is very good, especially for the degraded samples. As for materials of poor quality (i.e., low-temperature material in the degraded state) the cell performances are mainly governed by strong recombination losses in the intrinsic layer, a good correlation for those samples is obtained here. On the other hand, for high-quality material with  $\mu^0\tau^0$  typically higher than  $1 \times 10^{-7} \text{ cm}^2/\text{V}$ , the influence of other loss mechanisms (e.g., interdiffusion at high deposition temperatures) gains importance and the cell performances are lower than what could be expected from the quality of the incorporated  $a\text{-Si:H}$  material (as measured by  $\mu^0\tau^0$ ).

Both in the annealed as well as in the degraded state, the  $\mu^0\tau^0$  products show a strong decrease with lower deposition temperatures which can be seen only in a weakened form by CPM deep defect density measurements. We attribute this discrepancy to a lower band mobility in these low-temperature films. In fact, the reduced values for electron band mobilities in low-temperature  $a\text{-Si:H}$  have been recently confirmed, for one series of samples discussed here, using transient measurement techniques.<sup>26</sup> One may be lead to infer from the arguments used in Sec. II A (to justify theoretically the equality of the two  $\mu^0\tau^0$  products for holes and electrons), that in layers of different structural disorder  $\mu^0\tau^0$  should only depend on the deep defect density (and the capture cross sections) and not on the variation in band mobilities,<sup>27</sup> however, our experimental data do not confirm such conclusion.

## V. CONCLUSIONS

In this article we have presented and discussed in detail a new method to deduce from experimental steady-state  $\mu\tau$  measurements (by the steady-state photoconductivity and steady-state photocarrier grating techniques) more relevant information about the quality of  $a\text{-Si:H}$  layers. To this end, a new parameter called  $\mu^0\tau^0$  has been introduced. This  $\mu^0\tau^0$  product monitors the quality of the material in terms of band mobility and deep defect density, it does not depend, as the experimental  $\mu\tau$  products do, on the actual dangling bond occupation (charge state) prevailing in the measured sample.

The evaluation of  $\mu^0\tau^0$  products on a series of undoped and slightly doped  $a\text{-Si:H}$  films allowed us to estimate the value of the ratio of dangling bond capture cross sections  $\sigma^{\pm}/\sigma^0 \approx 50$ .

As the evaluated  $\mu^0\tau^0$  product, containing information about the band mobility and the defect density, is closely related to the internal collection, and, thus, in principle, to the efficiency of  $a\text{-Si:H}$   $p\text{-i-n}$  solar cells, we propose that one should in future use  $\mu^0\tau^0$  products as a tool for material optimization in view of improving the quality of the intrinsic layer within  $p\text{-i-n}$  solar cells. Thereby—as presented in Table I—the evaluation of  $\mu^0\tau^0$  from experimental data becomes particularly simple in most cases: In all  $a\text{-Si:H}$  layers with an extrinsic character material quality is monitored by the ambipolar diffusion length  $L_{\text{amb}}$ , whereas in midgap  $a\text{-Si:H}$  layers it is the photoconductivity which monitors correctly the material quality.

We have obtained a good correlation between the  $\mu^0\tau^0$  products measured on  $a\text{-Si:H}$  films (and evaluated in the manner described here), on one side, and the performances

of solar cells incorporating the same material as an active  $\langle i \rangle$  layer, on the other side. However, one has to keep in mind the complexity of a solar cell device (which includes doped layers, contacts, interfaces); thus, our new  $\mu^0\tau^0$  product may only be used to optimize solar cell performances as far as the intrinsic layer is concerned.

A problem for further investigation is the possible anisotropy of  $a$ -Si:H layers. In fact, the evaluation of the  $\mu^0\tau^0$  product is based on measurements done in a coplanar configuration, whereas the  $p$ - $i$ - $n$  solar cell operates in a sandwich structure. For VHF glow discharge deposition of  $a$ -Si:H from pure silane (the deposition technique used for the present article), various tests have demonstrated that such an anisotropy is negligible, either by time of flight<sup>28</sup> or by small-angle x-ray scattering (SAXS)<sup>29</sup> measurements. However, in layers and cells produced by rf or microwave glow discharge under hydrogen dilution of silane, a pronounced anisotropy is generally observed by SAXS measurements<sup>30</sup> which could possibly lead to an anisotropy of the transport properties. This, indeed, constitutes a problem which should be addressed in the future.

## ACKNOWLEDGMENTS

The authors would like to acknowledge the help of S. Dubail for the sample preparation, as well as the financial support from the Swiss Federal Renewable Energy Program [EF-REN(93)032] and from the Swiss National Science Foundation Grant No. FN-39377.

<sup>1</sup>C. Wronski, R. M. Dawson, M. Gunes, Y. M. Li, and R. W. Collins, MRS Proc. **297**, 443 (1993).

<sup>2</sup>R. E. I. Schropp, A. Sluiter, M. B. von der Linden, and J. Daey Ouwens, J. Non-Cryst. Solids **164-166**, 709 (1993).

<sup>3</sup>J. Yang, X. Xu, and S. Guha, MRS Proc. **336**, 687 (1994).

<sup>4</sup>T. Nishiwaki and S. Nitta, Philos. Mag. B **69**, 335 (1994).

<sup>5</sup>A. Mettler, N. Wyrsh, M. Goetz, and A. Shah, Sol. Energy Mater. Sol. Cells **34**, 533 (1994).

<sup>6</sup>M. S. Brandt and M. Stutzmann, J. Non-Cryst. Solids **137&138**, 211 (1991).

<sup>7</sup>N. Hata, I. S. Osborne, T. Ikeda, R. Durny, and A. Matsuda, J. Non-Cryst. Solids (to be published).

<sup>8</sup>R. A. Street, J. Zesch, and M. J. Thompson, Appl. Phys. Lett. **43**, 672 (1983).

<sup>9</sup>N. Beck, N. Wyrsh, E. Sauvain, and A. Shah, MRS Proc. **297**, 479 (1993).

<sup>10</sup>L. Yang, A. Catalano, R. R. Arya, M. S. Bennett, and I. Balberg, MRS Proc. **149**, 563 (1989).

<sup>11</sup>N. Beck, A. Shah, and N. Wyrsh, in Proceedings, of the 1st WCPEC, Hawaii 1994, p. 476.

<sup>12</sup>F. Vaillant and D. Jousse, Phys. Rev. B **34**, 4088 (1986).

<sup>13</sup>J. Hubin, A. Shah, and E. Sauvain, Philos. Mag. Lett. **66**, 115 (1992).

<sup>14</sup>N. Beck, N. Wyrsh, E. Sauvain, and A. Shah, in Proceedings of the 11th ECPVSEC 1992, p. 625.

<sup>15</sup>R. S. Crandall, Semiconductors and Semimetals B **21**, 245 (1984).

<sup>16</sup>D. Ritter, K. Weiser, and E. Zeldov, J. Appl. Phys. **62**, 4563 (1987).

<sup>17</sup>A. Shah, J. Hubin, E. Sauvain, P. Pipoz, N. Beck, and N. Wyrsh, J. Non-Cryst. Solids **164-166**, 485 (1993).

<sup>18</sup>K. Hattori, Y. Niwano, H. Okamoto, and Y. Hamakawa, J. Non-Cryst. Solids **137&138**, 363 (1991).

<sup>19</sup>M. Günes, R. W. Collins, and C. R. Wronski, MRS Proc. **336**, 413 (1994).

<sup>20</sup>N. Wyrsh and A. Shah, J. Non-Cryst. Solids **137&138**, 431 (1991).

<sup>21</sup>N. Wyrsh and A. Shah, Solid State Commun. **80**, 807 (1991).

<sup>22</sup>H. Curtins, N. Wyrsh, M. Favre, and A. Shah, Plasma Chem. Plasma Proc. **7**, 267 (1987).

<sup>23</sup>R. A. Street, *Hydrogenated Amorphous Silicon* (Cambridge University Press, Cambridge, 1991), pp. 136 and 147.

<sup>24</sup>Y.-M. Li, MRS Proc. **297**, 803 (1993).

<sup>25</sup>J. H. Zhou and S. R. Elliott, Philos. Mag. B **69**, 147 (1992).

<sup>26</sup>M. Goerlitzer, P. Pipoz, H. Beck, N. Wyrsh, and A. Shah, MRS Proc. **377**, 503 (1995).

<sup>27</sup>N. F. Mott and E. A. Davis, *Electronic Processes in Noncrystalline Materials* (Clarendon, Oxford, 1979).

<sup>28</sup>J. Kočka, E. Šípek, O. Štika, H. Curtins, and G. Juška, J. Non-Cryst. Solids **114**, 336 (1989).

<sup>29</sup>S. J. Jones, Y. Chen, D. L. Williamson, U. Kroll, and P. Roca i Cabarrocas, J. Non-Cryst. Solids **164&166**, 131 (1993).

<sup>30</sup>S. Guha (private communication).